



Cite this: *Phys. Chem. Chem. Phys.*,
2024, 26, 2815

Natural resonance-theoretic conceptions of extreme electronic delocalization in soft materials†

Frank Weinhold ^a and Eric D. Glendening ^b

In the broad context of Dalton's atomic hypothesis and subsequent classical vs. quantum understanding of macroscopic materials, we show how Pauling's resonance-type conceptions, as quantified in natural resonance theory (NRT) analysis of modern wavefunctions, can be modified to unify description of interatomic interactions from the Lewis-like limit of localized e-pair covalency in molecules to the extreme delocalized limit of supramolecular "soft matter" aggregation. Such "NRT-centric" integration of NRT bond orders for hard- and soft-matter interactions is illustrated with application to a long-predicted and recently synthesized organometallic sandwich-type complex ("diberyllocene") that exhibits bond orders ranging from the soft limit ($b_{BeC} \approx 0.01$) to the typical values ($b_{CC} \approx 1.35$) of molecular resonance-covalency in the organic domain, with intermediate value ($b_{BeBe} \approx 0.86$) for intermetallic $Be\cdots Be$ interaction.

Received 3rd October 2023,
Accepted 28th December 2023

DOI: 10.1039/d3cp04790c

rsc.li/pccp

Introduction: quantal vs. classical conceptions of soft matter interactions

In reconsidering prevailing general conceptions concerning molecules and materials, it is appropriate to briefly reflect on the historical sequence by which present "physical" conceptions of chemical behavior were achieved.

Speculations on the atomic-level nature of matter trace back to antiquity,¹ but firm scientific foundations for atomistic conceptions, building on the systematic weight measurements of Lavoisier² and Dalton³ and rational theoretical formulations of Gibbs,⁴ offered ever-increasing support for Boltzmann's boldly literal conjectures concerning the "moving material points" (atoms and molecules) that underlie macroscopic chemical, electrical, and thermal phenomena.⁵

In the early 20th century, more detailed electronic (e-level) conceptions of chemical bonding between atoms were spurred particularly by Lewis's dot-diagrams depicting localized e-pair-sharing ("covalency") between the valence-shell electrons of the Z -charged nucleus of each neutral atom.⁶ Planck's discovery⁷ of the quantum of action (\hbar) was subsequently recognized by Bohr⁸ as providing quantitative explanation for the spectral

lines of hydrogen ($Z = 1$) as well as compelling rationale for the periodicity patterns in Mendeleev's table of chemical elements for higher Z .⁹

These revolutionary developments culminated in the 1925–1926 papers of Heisenberg,¹⁰ Schrödinger,¹¹ and Dirac.¹² All available results from precision comparisons of theory and experiment¹³ support the claim that the properties of all chemical species (implicitly including those of biological, agricultural, and geological interest, and many yet to be discovered) are correctly described by the equations of quantum mechanics, both in non-relativistic^{10,11} and relativistic¹² limits. The quantum mechanical equations thus supersede all classical-mechanical frameworks as proper foundation for the deepest conceptions of the materials domain.

Contrary to the above statement, some workers continue to argue that "quantum effects" extend only to the covalent e-pairing interactions of molecule formation, whereas the soft "noncovalent" attractions (e.g., of ligation or complexation) are to be rationalized in terms of classical electrostatic conceptions of dipole–dipole or higher multipole type. In this view, quantum equations are reserved for the "hard" interactions of molecular single-, double-, triple-bond formation, with intermediate fractional values attributable to weaker resonance-type corrections, whereas interactions of the intermolecular domain can be adequately "simulated" with molecular dynamics (MD) equations of purely classical form, thereby avoiding the complexities of exchange, superposition, and related orbital-type features of the molecular regime.

However, any such presumption of separable "covalent vs. noncovalent" (or "intramolecular vs. intermolecular,"

^a Theoretical Chemistry Institute and Department of Chemistry, University of Wisconsin-Madison, Madison, WI 53706, USA. E-mail: weinhold@chem.wisc.edu

^b Department of Chemistry and Physics, Indiana State University, Terre Haute, IN 47809, USA. E-mail: eric.glendening@indstate.edu

† Electronic supplementary information (ESI) available. See DOI: <https://doi.org/10.1039/d3cp04790c>

“covalent *vs.* ionic,” *etc.*) bonding represents a false dichotomy in the logical sense. Such dichotomy would erroneously suggest that disjoint aspects of chemical behavior can be evaluated by mutually inconsistent mathematical assumptions and simply added together (in the style of “energy decomposition analysis” schemes¹⁴) to obtain successful theoretical predictions of material properties.

According to Bohr’s correspondence principle,¹⁵ proper quantum equations must automatically reduce to their classical counterpart in the limit of large quantum numbers or vanishing quantum of action ($\hbar \rightarrow 0$). This implies that the quantum equations already include all relevant contributions of classical type, rather than requiring addition of separate “quantal” and “classical” contributions to total energy.

Aside from these formal considerations, one can look at the historical record of atomistic-level classical-MD methods in attempts to solve substantive scientific problems. Perhaps most famous (or infamous) in this respect is the protein-folding problem, formalized over nearly 30 years in the biennial CASP (“Critical Assessment of Structure Prediction”) competition co-founded by computational biologist John Moult.¹⁶ Each new CASP event featured a newly chosen protein whose native folded structure had been recently determined by X-ray crystallography, but with structural coordinates withheld from public distribution. Competing MD specialists were provided with the primary amino acid sequence, and all have access to the many previously determined native protein structures. Each competitor then employs a favored MD force field to computationally “predict” the correctly folded protein structure, usually with profoundly disappointing results for all concerned.

However, as recently reported,¹⁶ a new artificial-intelligence (AI) competitor AlphaFold swept the 2020 competition with essentially perfect results, even though it has nothing in common with atomistic-level MD simulations! Magically, AlphaFold was able to solve the problem simply by using AI pattern-recognition algorithms on the widely available crystallographic database of previously solved structures. The combined efforts of 30+ years of classical-MD simulations therefore appear to have contributed less than “nothing” to the eventual successful predictions of protein-folding. “In some sense the problem is solved,” said Moult. However, the same classical-based MD conceptions that failed to properly predict protein folding can hardly be expected to correctly predict the chemical functionality of the folded structures as now provided by AlphaFold or experiment. Human scientists have no more insight than before about how and why proteins fold and function as they do.

Our goal here is to urge precedence for theoretical studies of materials that are firmly based on authentic quantum chemical methods and the conceptual insights they provide through the lens of natural bond orbital (NBO)¹⁷ and natural resonance theory (NRT)¹⁸ analysis. Throughout this discussion, we focus primarily on the neutral closed-shell ground states of common laboratory substances. All NBO/NRT methods rest on Löwdin’s “natural” orbital conceptions,¹⁹ which in turn originate in von

Neumann’s density operator ($\hat{\Gamma}$) formulation of quantum mechanics²⁰ for a specific state Ψ of the N -electron system. In Dirac notation, $\hat{\Gamma}$ is expressed as the integral operator

$$\hat{\Gamma} = |\Psi\rangle\langle\Psi| \quad (1)$$

with kernel

$$\Gamma(1,2,\dots,N|1',2',\dots,N') = \Psi(1,2,\dots,N)\Psi^*(1',2',\dots,N') \quad (2)$$

The intrinsic electronic indistinguishability guaranteed by the Pauli exclusion principle then allows one to evaluate exact 1e-properties (additive operators of 1-electron type, such as kinetic energy, Coulombic attraction to nuclei, dipole moment, total e-density at point \mathbf{r} , *etc.*) from the reduced density operator (“1-matrix”) $\hat{\Gamma}^{(1)}$, with kernel

$$\Gamma^{(1)}(1|1') = N \int \Gamma(1,2,\dots,N|1',2,\dots,N) d2 d3 \dots dN \quad (3)$$

(and similarly, 2e properties such as interelectron Coulomb repulsion from the corresponding 2-matrix $\hat{\Gamma}^{(2)}$, *etc.*).

In a chosen spin-orbital basis $\{\chi_k\}$, the “density matrix” representation (\mathbf{D}) of $\hat{\Gamma}^{(1)}$ has elements

$$(\mathbf{D})_{jk} = \langle \chi_j | \hat{\Gamma}^{(1)} | \chi_k \rangle \quad (4)$$

Löwdin showed that the eigenorbitals (“natural” orbitals; NOS) of \mathbf{D} have maximum occupancy properties that ensure their optimal term-by-term convergence (compared to any alternative orthonormal set) in representing the e-density of the chosen system and state. The corresponding localized natural atomic orbitals (NAOs $\{\theta_k^{(A)}\}$) and natural bond orbitals (NBOs $\{\Omega_k^{(AB)}\}$) are similarly obtained as eigenorbitals of atomic sub-blocks of \mathbf{D} , thereby inheriting similar optimal properties for representing 1/2-center (1c/2c) “lone pair” or “bond” contributions to total e-density. At the full N_e -level, the NRT “resonance structures” are each composed from optimized NBOs of the associated bonding pattern, with convex-optimized weightings to guarantee maximum resemblance of the NRT expansion to overall e-density. Further details of NBO/NRT origins and usage are described elsewhere.²¹

NBO/NRT methods are implemented in a widely used computer program (currently NBO 7.0)²² that can be interactively linked with a wide variety of popular electronic structure systems,²³ insuring strict consistency of theoretical descriptors across a broad selection of quantum chemical methods [semi-empirical, HF, DFT, MP(n), CI, CC(SDT...), CASSCF,...] and basis sets [Gaussian, Slater, or implicit (semi-empirical) AOs] in common usage.²⁴

In the ensuing discussion, we first outline the extremes of localization and delocalization that are found in NBO/NRT studies across the periodic table. We then focus on the characteristic features of NRT description in the case of species of weak vibrational rigidity, dissociation energy, or thermal stability (evidence of mechanical “softness”) or high electrical and thermal conductivity (evidence of electronic “delocalization”). In each case we employ NRT interatomic bond orders $\{b_{AB}\}$ as primary theoretical descriptors of localized bonding strength, expected to serve as principal theoretical correlators with

experimentally measurable bond properties such as bond length (R_{AB}), bond dissociation energy ($\Delta E_{A\cdots B}$), bond vibrational frequency (ν_{AB}), NMR coupling ($^1J_{AB}$), and the like. Our goal is thereby to further broaden the NBO/NRT framework to deal with the more extreme delocalization effects in materials that lack conventional “molecule-like” connectivity.

Localized and delocalized extremes of chemical bonding

Electronic structure theory advanced rapidly in the years immediately following discovery of the Schrödinger equation. Early numerical applications of molecular orbital (MO) theory to the hydrogen molecular ion²⁵ and valence bond (VB) theory to the hydrogen molecule²⁶ soon led to Pauling's masterful “nature of the chemical bond” exposition of hybridization and resonance concepts, initially in a series of papers²⁷ and subsequently in the famous book²⁸ that “brought quantum mechanics into practical chemistry” and has been compared with Newton's *Principia* and Darwin's *Origin of Species* for its iconic status in the development of scientific thought.²⁹

Pauling's VB-style empiricism was chosen to map directly onto G. N. Lewis's dot-diagrams⁶ depicting the shared e-pairs that underlie the localized interatomic “sticks” of covalent bonding to form molecules. In what came to be identified as the HLSP-PP-VB (Heitler–London–Slater–Pauling perfect-pairing valence bond) formulation,³⁰ each localized σ_{AB} bond of the skeletal framework is composed from overlapping sp^n -type directed hybrid orbitals (h_A , h_B) on the bonding atoms. In VB-representation, the spatial factor of each 2-center/2-electron (2c/2e) wavefunction is taken to be of the form

$$\sigma_{AB}^{(VB)}(1,2) = 2^{-1/2}[h_A(1)h_B(2) + h_B(1)h_A(2)] \quad (5)$$

However, this functional form is inflexibly homopolar, whereas the more adaptable “bond orbital” form suggested by Mulliken³¹ retains the idea of atomic hybridization but rewrites the spatial 2c/2e wavefunction in factored form as

$$\sigma_{AB}^{(BO)}(1,2) = [c_A h_A(1) + c_B h_B(1)][c_A h_A(2) + c_B h_B(2)] \quad (6a)$$

with polarization coefficients c_A , c_B satisfying the normalization condition

$$|c_A|^2 + |c_B|^2 = 1 \quad (6b)$$

whichever form is preferred, the restriction to hybrids h_A , h_B drawn only from the complete set of atomic orbitals (AOs) on centers A, B insures the complete localization of the e-pair on these centers.

Pauling's resonance concept was introduced to deal with benzene and similar exceptional cases where the Lewis electron-dot mnemonic requires a pattern of alternating single- and double-bonds, but the experimental structure is of higher symmetry (e.g., D_{6h} for actual benzene *vs.* D_{3h} for Lewis-structural “cyclohexatriene”). In such cases, the actual many-electron wavefunction Ψ is envisioned as a “resonance hybrid”

of the two alternative localized Lewis-structural patterns Φ_I , Φ_{II} , which can be expressed in von Neumann's density-operator notation (1) as

$$\hat{\Gamma}_{NRT} = w_I |\Phi_I\rangle\langle\Phi_I| + w_{II} |\Phi_{II}\rangle\langle\Phi_{II}| \quad (7a)$$

with non-negative weightings summing to unity

$$w_I + w_{II} = 1 \quad (7b)$$

NRT optimization serves to maximize the non-negative variational functional

$$\langle \Psi | \hat{\Gamma}_{NRT} | \Psi \rangle = \langle \Psi | [w_I |\Phi_I\rangle\langle\Phi_I| + w_{II} |\Phi_{II}\rangle\langle\Phi_{II}|] | \Psi \rangle = \max \quad (8)$$

that ensures best-possible “resemblance” between $\hat{\Gamma}$ and $\hat{\Gamma}_{NRT}$. The convex form (7a) for density-based optimizations may be contrasted with the corresponding configuration interaction (CI) form for energy-based optimizations, with superposition coefficients of either sign and multiple cross-terms contributing to the target variational functional.

In benzene or other strongly conjugated molecules, the weightings w_I , w_{II} approach the symmetry-enforced limit ($w_I \approx w_{II} \approx 0.5$), but in the weaker resonance of amides or the still weaker cases of hyperconjugation,³² the weightings shift increasingly toward the near-Lewis-structure limit ($w_I \approx 1$, $w_{II} \approx 0$) of resonance-free bonding. Because each such resonance effect involves a type of “mixing” (delocalization) of the original 2c e-pair with another e-pair situated (partially or wholly) at a 3rd center, it is commonly identified as “3c/4e” (partially delocalized) bonding, thereby distinguished from conventional 2c/2e bonding of a fully localized Lewis-structural bonding pattern.

Note that NRT methods can also be applied to open-shell radicals or excited-state species to study the delocalized spin distributions and related magnetic properties. However, the NRT bonding patterns of a given system and state are only “precursors” to possible low-barrier reactive pathways for forming bond-shifted products, or envisioned multi-state “quasi-particle” excitation phenomena of condensed phases. Furthermore, current NBO/NRT methodology applies only to fixed- N species, rather than infinitely extended models for condensed phases.

In most respects, NRT results closely mirror Pauling's original resonance concepts,³³ but with two important exceptions:

(i) The numerical NRT weightings $\{w_r\}$ are determined from a rigorous “maximum density” criterion (analogous to that used to determine the hybridization and polarization properties of NBOs) rather than the empirical fitting to measured structural parameters as adopted by Pauling;

(ii) NRT bond orders can in principle acquire non-negative fractional values anywhere from zero upward, whereas Pauling's original resonance-mixing applied only to intramolecular interactions, thereby yielding fractional values only between positive integer (single, double, triple,...) bonds of the molecular skeleton (as judged from empirical covalent radii for each atom).

However, from the many short contact distances that were found between non-bonded atoms in the 40-plus years since his original resonance conceptions, Pauling later recognized³⁴ that resonance-type stabilization must extend to “no-bond resonance” of the intermolecular domain in certain metallic cases. This concurs with the general NBO/NRT perception that quantum resonance-covalency (3c/4e donor–acceptor stabilization) extends into the regime of “soft” intermolecular interactions (with bond orders in the range $0 \leq b_{A \cdots B} \leq 1$, smoothly connecting with known intramolecular bond-order variations). In this respect, Pauling’s readjusted position on supramolecular resonance is closer to the early viewpoint of Sidgwick³⁵ and many subsequent workers, particularly for the H-bonding phenomenon.³⁶

In outline, the NRT program employs an iterative algorithm to generate a “tree” of candidate resonance structures from the initial NBO structure, as well as any other user-suggested structures that may be provided in \$NRTSTR keylist input.¹⁸ Successive iterative cycles then lead to many such candidate bonding patterns (possibly tens of thousands!) that might seem to present an insuperable numerical task for the weightings-optimizer. However, the intrinsic “convex programming”³⁷ mathematical structure of the optimization problem ensures that the final weightings are generated in robustly stable and efficient fashion with full numerical accuracy.^{18d}

Resonance primacy: the other side of the localization coin

Historically, the development of electronic bonding concepts, as well as the original NBO program itself, was dominated by G. N. Lewis’s seminal recognition of localized 2c/2e “pairing” as the primary feature of chemical bonding. In this limit, the iconic ball-and-stick picture of molecular connectivity in some “primary” bonding pattern becomes the starting point for perturbative evaluation of “secondary” resonance-type delocalization effects. In the present *NBO7* program, the primacy of the natural Lewis structure (NLS) bonding pattern is implicitly assumed, and indeed, the combined sum of secondary NRT-type corrections is commonly less than that of the primary NLS contribution in organic main-group applications. [Note that the corrupted and obsolete “NBO 3.1” program distributed with *Gaussian-16* has no authentic NRT capability, even though it contains code that apparently reads NRT-related keyword input.]

However, with a robustly general NRT search algorithm in hand, it becomes feasible to envision an alternative NRT-centric analysis designed for an entirely different domain of electronic delocalization effects, as well as smooth reduction to the NLS-centric limit. In such NRT-centric formulation, the formal NLS bonding pattern may play little or no role as “parent” for generation of trial structures to be included in variational optimization of NRT weightings. Far from being “primary” or “dominant,” the formal NLS may have negligible weighting in the final NRT expansion, which instead represents

an extended delocalization network with no single bonding pattern achieving the significant majority weighting to warrant ball-and-stick (molecule-like) preferential status. In some respects, this is analogous to the way in which a particular free-atom valence-shell NAO may become a small minority contributor to the more general natural hybrid orbital (NHO) that better serves as conceptual building-block for the network of covalent bonds in a Lewis-structural bonding pattern.

For specificity, we identify the leading (highest weighted) structure of the NRT expansion as the “natural resonance-type Lewis-structure” (NRLS) to distinguish it (if necessary) from the NBO-centric NLS. In the extreme NRT-centric limit, only the final bond orders (many or all in the $0 < b_{AB} < 1$ range) remain as useful “local” descriptors of resonance-type stabilization that correlate with structural bond lengths or other measurable interatomic properties. Of course, many intermediate cases can occur between the envisioned extreme limits of NLS-centric (“localized Lewis-like”) and NRT-centric (“completely delocalized”) electronic behavior, but a properly generalized NBO/NRT analysis framework should be able to range freely between these “hard” ($b_{AB} > 1$) and “soft” ($b_{AB} \rightarrow 0$) limits of material behavior.

In the present work, we employ a simple “intermediate” example of resonance delocalization in a sandwich-type organometallic complex (diberyllocene) to illustrate how the present *NBO 7.0* algorithms can be extended toward the NRT-centric limit of “extreme” delocalization in metallic or soft-matter species. In this intermediate-delocalization case, the default NRT search is found to be adequate, but the illustrated protocol serves to ensure “completeness” of the NRT search for contributing structures. In future NBO program versions, the illustrated strategy (involving use of \$CHOOSE and \$NRTSTR keylists) will be automated to ensure consistency between the final NRLS bonding pattern of highest NRT weighting and the starting point for the recursive “tree” of NRT-guess structures for which optimized weightings are computed.

Illustrative application to diberyllocene

As an example of current research interest, we illustrate the NRT-centric approach to analyzing the delocalization in diberyllocene, $(\text{BeC}_5\text{H}_5)_2$, a surprising sandwich-like organometallic complex with cyclopentadienyl groups encapsulating what is nominally a dimer of beryllium ($Z = 4$), a notoriously poisonous element with known aversion to forming dimetallic Be–Be bonds. The structural details of diberyllocene (including the curiously eclipsed C_{5h} geometry) were first predicted theoretically by the Schaefer group in 2005,³⁸ but a successful synthesis and X-ray characterization was achieved only recently,³⁹ heralded as “A big breakthrough for beryllium.”⁴⁰

A variety of *ab initio* and DFT methods and basis sets are found to yield satisfactory agreement with the experimental X-ray structure for diberyllocene. For present purposes we employ a simple B3LYP/6-311++G** level of hybrid density functional theory, which allows direct comparison with NBO/

Table 1 Comparison of selected diberyllocene bond lengths R_{AB} (Å) and CH-bending angles ($^\circ$) in the earlier prediction³⁸ with those of the present work

Geometry	Ref. 38	Present
$R_{C(1)Be(21)}$	1.968	1.952
$R_{C(1)C(2)}$	1.425	1.418
$R_{C(1)H(6)}$	1.085	1.079
$R_{Be(21)Be(22)}$	2.057	2.041
$\Delta_{x-C(1)-H(6)}$	3.4°	3.2°

NRT results for many other chemical species.³⁶ Table 1 compares calculated B3LYP/6-311++G** structural parameters with those of the earlier theoretical prediction,³⁸ both in close agreement with the recent X-ray measurements.³⁷

Diberyllocene exemplifies a dilemma of the original NRT implementation¹⁸ that occurs whenever the “leading” (NRLS) structure of the NRT expansion is inconsistent with the supposedly “best” (NLS) single Lewis structure (according to the variational maximum-density criterion by which NBO algorithms

are governed¹⁷). This inconsistency is uncommon in the vast majority of stable chemical compounds to be found in the chemical laboratory and discussed in chemistry classrooms. However, examples of such NLS/NRLS mismatch become increasingly common in the “soft-matter” domain of weak supramolecular interactions, where no interatomic bond order may reach the threshold ($b_{AB} \geq 1$) considered necessary for “molecule” formation.

Given the NLS *vs.* NRLS distinction, we can recognize that the choice of NLS as starting point for NRT-based studies of resonance phenomena is a rather arbitrary consequence of the bias introduced by historical sequence, with general recognition of “Lewis structure” preceding that of multi-structural “resonance” by more than a decade. The variational NRT algorithm (7) is the appropriate generalization of the self-same maximum-density criterion that governs all “natural” orbital concepts.¹⁹ As indicated above, multi-reference NRT is manifestly more general than single-NLS description. Accordingly, both logical and numerical consistency demand that the

(a)																					
LONE 1 1 14 1 END																					
BOND S 1 2 S 1 5 S 1 6 D 2 3 S 2 7 S 3 4 S 3 8 D 4 5 S 4 9 S 5 5 10 S 11 12																					
D 11 15 S 11 16 D 12 13 S 12 17 S 13 14 S 13 18 S 14 15 S 14 19 S 15 20																					
S 21 22 END																					
(b)																					
cycle	structures	D(w)	kmax	CHOOSE	ION	CULL	E2	SYM	dbmax	dbrms											
1	1/1	0.09256740	1	64	0	0	132	0	2.000	1.254											
2	12/143	0.06757417	14	8064	-14	0	1066	0	0.410	0.208											
3	44/2139	0.06158282	63	92164	-428	0	1004	0	0.220	0.111											
4	120/2135	0.06082179	187	60416	-1188	0	1008	0	0.081	0.040											
5	231/2923	0.06082137	160	61440	-432	0	1078	0	0.000	0.000											
6	223/4737	0.06078101	151	62404	-492	0	0	0	0.014	0.005											
(c)																					
STR	! Wgt=2.67%; rhoNL=2.86360; D(0)=0.09257																				
LONE	5 1 15 1 END																				
BOND	D 1 2 S 1 5 S 1 6 S 2 3 S 2 7 D 3 4 S 3 8 S 4 5 S 4 9 S 5 5 10																				
	D 11 12 S 11 15 S 11 16 S 12 13 S 12 17 D 13 14 S 13 18 S 14 15																				
	S 14 19 S 15 20 S 21 22 END																				
END																					
(d)																					
\$CHOOSE																					
LONE	5 1 15 1 END																				
BOND	D 1 2 S 1 5 S 1 6 S 2 3 S 2 7 D 3 4 S 3 8 S 4 5 S 4 9 S 5 5 10																				
	D 11 12 S 11 15 S 11 16 S 12 13 S 12 17 D 13 14 S 13 18 S 14 15																				
	S 14 19 S 15 20 S 21 22 END																				
\$END																					
(e)																					
cycle	structures	D(w)	kmax	CHOOSE	ION	CULL	E2	SYM	dbmax	dbrms											
1	1/1	0.09257058	1	64	0	0	132	0	2.000	1.254											
2	12/143	0.06757531	14	8064	-14	0	1066	0	0.410	0.208											
3	44/2139	0.06158316	63	92164	-428	0	1004	0	0.220	0.111											
4	120/2135	0.06082177	187	60416	-1188	0	1008	0	0.081	0.040											
5	231/2923	0.06082134	160	61440	-432	0	1078	0	0.000	0.000											
6	223/4737	0.06078096	151	62404	-492	0	0	0	0.014	0.005											

Fig. 1 Details of NRLS-based NRT analysis for diberyllocene (see text), showing alternative starting structures [NLS (a) vs. NRLS (c)], \$CHOOSE input for the latter [(d)], and respective NRT search summaries [(b) and (e)].

former NRT algorithm be iteratively extended (if NLS and NRLS fail to coincide) with the NRLS (as obtained from initial NLS-based iteration) chosen as the starting point for full NRT re-optimization. This added step ensures self-consistency between initial and final assessment of which resonance structure is considered “best” in the more general NRLS-based framework. Such NRLS-based bond orders can be obtained by simply inserting the NRLS structure found in an initial NLS-based NRT search as \$CHOOSE keylist input (replacing the NLS) in a subsequent NRLS-based NRT search.

Fig. 1(a)–(e) shows further details of how NRLS-based NRT analysis is performed for diberyllocene. Fig. 1(a) shows details of the NLS bonding pattern that initiates the default NRT search [with LONE pairs on atoms 1, 14 and BOND pairs “S 1 2” (single bond between atoms 1, 2), “S 1 5” (single bond between atoms 1, 5), and so forth]. Fig. 1(b) shows the brief output summary of iterative cycles for the NLS-based search, which successively reduces overall $D(w)$ “error” by about 34% (from initial 0.09257 in cycle 1 to final 0.06078 in cycle 6) and leads to a final 223-term NRT expansion (out of 4737 trial structures considered). Fig. 1(c) shows details of the resulting NRLS bonding pattern that is highest-weighted ($w_1 = 2.67\%$) in the initial NRT search [with LONE pairs on atoms 5, 15 and BOND pairs “D 1 2” (double bond between atoms 1 and 2), “S 1 5” (single bond between atoms 1 and 5), and so forth], all differing from the NLS bonding pattern in Fig. 1(a). Fig. 1(d) shows how the NRLS bonding pattern is inserted in a \$CHOOSE...\$END keylist as input (to replace the NLS) in a new NRLS-based NRT search. Finally, Fig. 1(e) presents the summary of the alternative NRLS-based NRT search, which may be compared with the NLS-based search in Fig. 1(b).

In the present case, the NLS and NRLS are merely symmetry-equivalent alternatives, so the final NRLS-based NRT bond orders are identical to those of the default NLS-based search. However, this extra step gives insurance that no untapped reservoir of contributing resonance structures has been overlooked. It also justifies confidence that the calculated NRT bond orders are well converged and suitable for the intended correlations with measurable properties, a unique feature of bond-order measures compared to theoretical descriptors from other analysis methodologies.

Fig. 2 displays the optimized structure and NRLS-based NRT bond orders of diberyllocene at the B3LYP/6-311++G** level. The structure shows the striking D_{5h} symmetry of the complex, the curious eclipsed conformation of the two opposed Cp rings, and the barely perceptible inward “tilt” of CH bonds on each Cp ring toward the opposite face of the sandwich, all calling for electronic explanation.

Noteworthy in the present context is the distribution of NRT bond orders in Fig. 2, with “molecule-like” values ($b_{AB} \geq 1$) restricted to CC bonds of the capping cyclopentadienyl groups, whereas each Be atom engages only in distinctly sub-molecular bonding [$b_{BeBe} = 0.862$, $b_{BeC} = 0.014$] to adjacent atoms of the sandwich complex. Quantitative NBO/NRT descriptors also show sharp departures from ionic-type $[Cp^- \cdots Be^+ \cdots Be^+ \cdots Cp^-]$ conception. The natural population analysis (NPA) atomic charge

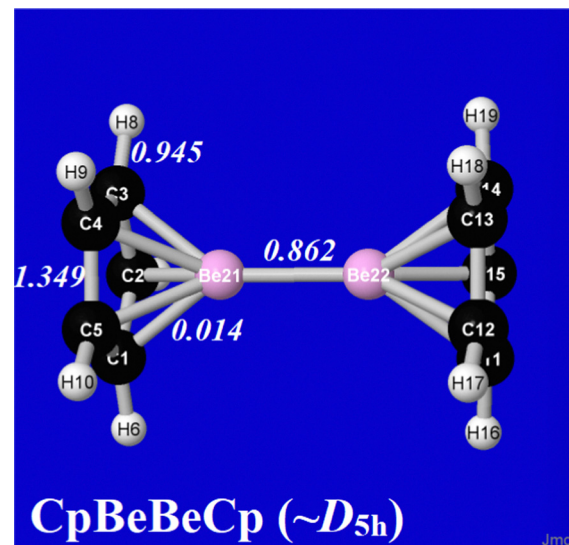


Fig. 2 NRT bond orders for the optimized B3LYP/6-311++G** structure of $(C_5H_5Be)_2$ of the present work.

($Q_{Be}^{(NPA)} = 0.84$) falls significantly below that of the formal “Be(I)” oxidation state of an ionic description. However, the authors of ref. 39 attribute this discrepancy to the fact that NPA charges “do not take into account the presence of the non-nuclear attractor” of the corresponding Bader-type “quantum theory of atoms in molecules” (QTAIM) value ($Q_{Be}^{(QTAIM)} = 1.39$). We believe that NBO/NRT charges and bond orders offer a more accurate and nuanced picture of bonding in diberyllocene than concepts based on the “non-nuclear attractor” artifacts of QTAIM partitioning.⁴¹

Concluding summary

We have sketched the outlines of an alternative “NRT-centric” formulation of NBO/NRT analysis methods that better ensures formal continuity of resonance-type bond-order descriptors that can range from the strongly localized Lewis-like limit of molecule formation (“hard” matter) to the strongly delocalized metallic-like limit of supramolecular (“soft” matter) interactions. Specific technical details of how such hard- → soft-matter transition can be accomplished in the framework of the current *NBO 7.0* analysis program are described and illustrated with application to a recently synthesized “diberyllocene” complex that promotes intermediate-type supramolecular Be···Be bonding in the sub-molecular ($b_{BeBe} < 1$) domain. Details of NBO/NRT analysis of diberyllocene exhibit the significant deviations from ionic-type $[Cp^- \cdots Be^+ \cdots Be^+ \cdots Cp^-]$ conceptions, as well as their alleged support from QTAIM-type descriptors.

The present application illustrates the case where no resonance structure acquires more than a small minority weighting (all $w_i < 3\%$), demonstrates the procedure to be followed whenever the leading structure of the NRT expansion differs from that of the starting NLS, and exhibits a variety of bond orders in the weak (b_{CBe}), intermediate (b_{BeBe}), and multiple-bonding (b_{CC}) range. However, the beryllocene sandwich-

complex, although interesting in other respects, is found to remain safely within the localized “molecule-like” range of the current NLS-based NRT search. Further exploration of the extreme delocalization limit therefore awaits NRT applications to transition-metal species with more characteristic metallic conduction and magnetic properties, as are expected to follow.

Conflicts of interest

There are no conflicts to declare.

References

- 1 Lucretius, *De Rerum Natura* (ca. 60 BC).
- 2 A. Lavoisier, *Traité Élémentaire de Chimie*, Paris, 1789.
- 3 J. Dalton, *A New System of Chemical Philosophy*, S. Russell, London, 1808.
- 4 (a) J. W. Gibbs, On the Equilibrium of Heterogeneous Substances, *Trans. Conn. Acad.*, 1874–1878, **3**, 108–248; (b) J. W. Gibbs, *Elementary Principles in Statistical Mechanics*, Charles Scribner's Sons, New York, 1902.
- 5 L. Boltzmann, Studien über das Gleichgewicht der lebendigen Kraft zwischen bewegeten materiellen Punkten, *Wien. Ber.*, 1868, vol. 58, pp. 517–560.
- 6 (a) G. N. Lewis, The Atom and the Molecule, *J. Am. Chem. Soc.*, 1916, **38**, 762–785; (b) G. N. Lewis, *Valence and the Nature of the Chemical Bond*, Chemical Catalog Co., New York, 1923.
- 7 M. Planck, Zur Theorie des Gesetzes der Energieverteilung im Normalspectrum, *Verh. Deut. Physik. Gesell.*, 1900, **2**, 202–204.
- 8 N. Bohr, On the Constitution of Atoms and Molecules, *Phil. Mag.*, 1913, **26**, 1–24.
- 9 V. Mendeleev, The Periodic Law of the Chemical Elements, *J. Chem. Soc.*, 1889, **55**, 634–656.
- 10 W. Heisenberg, Über quantentheoretische Umdeutung kinematischer und mechanischer Beziehungen, *Z. Phys.*, 1925, **33**, 879–893.
- 11 E. Schrödinger, Quantisierung als Eigenwertsproblem, *Ann. Phys.*, 1926, **384**, 361–376.
- 12 P. A. M. Dirac, On the Theory of Quantum Mechanics, *Proc. Roy. Soc. A*, 1926, **112**, 661–677.
- 13 For examples, see, e.g., H. Bethe and E. E. Salpeter, *Quantum Mechanics of One- and Two-Electron Atoms*, Springer, Berlin, 1957; H. F. Schaefer III, Methylen: A Paradigm for Computational Quantum Chemistry, *Science*, 1986, **231**, 1100–1107.
- 14 F. M. Bickelhaupt, C. F. Guerra, M. Mitoraj, F. Sagan, A. Michalak, S. Pan and G. Frenking, Clarifying Notes on the Bonding Analysis Adopted by the Energy Decomposition Analysis, *Phys. Chem. Chem. Phys.*, 2022, **24**, 15726–15735.
- 15 N. Bohr, Über die Serienspektren der Elemente, *Z. Phys.*, 1920, **2**, 423–478.
- 16 E. Callaway, After AlphaFold: Protein-Folding Contest Seeks Next Big Break-Through, *Nature*, 2023, **613**, 13–14.
- 17 F. Weinhold, The Path to Natural Bond Orbitals, *Isr. J. Chem.*, 2022, **62**, e202100026; F. Weinhold and C. R. Landis, *Discovering Chemistry with Natural Bond Orbitals*, John Wiley, Hoboken NJ, 2012.
- 18 (a) E. D. Glendening and F. Weinhold, Natural Resonance Theory. I. General Formulation, *J. Comput. Chem.*, 1998, **19**, 593–609; (b) E. D. Glendening and F. Weinhold, Natural Resonance Theory. II. Natural Bond Order and Valency, *J. Comput. Chem.*, 1998, **19**, 610–627; (c) E. D. Glendening, J. K. Badenhoop and F. Weinhold, Natural Resonance Theory. III. Chemical Applications, *J. Comput. Chem.*, 1998, **19**, 628–646; (d) E. D. Glendening, C. R. Landis and F. Weinhold, Resonance Theory Reboot, *J. Am. Chem. Soc.*, 2019, **141**, 4156–4166.
- 19 P.-O. Löwdin, Quantum Theory of Many-Particle Systems. I. Physical Interpretations by Means of Density Matrices, Natural Spin Orbitals, and Convergence Problems in the Method of Configurational Interaction, *Phys. Rev.*, 1955, **97**, 1474–1489.
- 20 J. von Neumann, *Mathematical Foundations of Quantum Mechanics*, Princeton University Press, Princeton NJ, 1955.
- 21 F. Weinhold, C. R. Landis and E. D. Glendening, What is NBO Analysis and How is it Useful?, *Int. Rev. Phys. Chem.*, 2016, **35**, 399–440.
- 22 E. D. Glendening, J. K. Badenhoop, A. E. Reed, J. E. Carpenter, J. A. Bohmann, C. M. Morales, P. Karafoglou, C. R. Landis and F. Weinhold, *NBO 7.0*, Theoretical Chemistry Institute, University Wisconsin, Madison, 2018, <https://nbo7.chem.wisc.edu/>.
- 23 NBO “Affiliated Programs” link: https://nbo7.chem.wisc.edu/affil_css.htm.
- 24 J. B. Foresman and Å Frisch, *Exploring Chemistry with Electronic Structure Methods*, Gaussian Inc., Wallingford CT, 2015.
- 25 L. Pauling, The Application of the Quantum Mechanics to the Structure of the Hydrogen Molecule and Hydrogen Molecule-Ion and to Related Problems, *Chem. Rev.*, 1928, **5**, 173–213.
- 26 W. Heitler and F. London, Wechselwirkung neutraler Atome und homopolar Bindung nach der Quantenmechanik, *Z. Phys.*, 1927, **44**, 455–472.
- 27 L. Pauling, The Nature of the Chemical Bond. Application of Results Obtained from the Quantum Mechanics and from a Theory of Paramagnetic Susceptibility to the Structure of Molecules, *J. Am. Chem. Soc.*, 1931, **53**, 1367–1400, and references therein.
- 28 L. Pauling, *The Nature of the Chemical Bond and the Structure of Molecules and Crystals*, Cornell University Press, Ithaca NY, 1939.
- 29 P. Ball, In Retrospect: Pauling's Primer, *Nature*, 2010, **468**, 1036.
- 30 G. A. Gallup, A Short History of Valence Bond Theory, in *Valence Bond Theory*, ed. D. L. Cooper, Elsevier, Amsterdam, 2002.
- 31 R. S. Mulliken, Electronic Structures of Polyatomic Molecules and Valence. II. General Considerations, *Phys. Rev.*, 1932, **41**, 49–71.

32 R. S. Mulliken, C. A. Rieke and W. G. Brown, Hyperconjugation, *J. Am. Chem. Soc.*, 1941, **63**, 41–56.

33 E. D. Glendening and F. Weinhold, Pauling's Conceptions of Hybridization and Resonance in Modern Quantum Chemistry, *Molecules*, 2021, **26**, 4110.

34 L. Pauling, Metal-Metal Bond Lengths in Complexes of Transition Metals, *Proc. Natl. Acad. Sci. U. S. A.*, 1976, **73**, 4290–4293.

35 N. V. Sidgwick, *The Electronic Theory of Valency*, Oxford University Press, London, 1929.

36 F. Weinhold and C. R. Landis, *Valency and Bonding*, Cambridge University Press, Cambridge UK, 2005.

37 J. Nocedal and S. Wright, *Numerical Optimization*, Springer, New York, 2nd edn, 2006; E. D. Glendening, S. J. Wright and F. Weinhold, Efficient Optimization of Natural Resonance Theory Weightings and Bond Orders by Gram-Based Convex Programming, *J. Comput. Chem.*, 2019, **40**, 2028–2035.

38 Y. Xie, H. F. Schaefer III and E. E. Jemnis, Characteristics of Novel Sandwiched Beryllium, Magnesium, and Calcium Dimers: $C_5H_5BeBeC_5H_5$, $C_5H_5MgMgC_5H_5$, and $C_5H_5CaCaC_5H_5$, *Chem. Phys. Lett.*, 2005, **402**, 414–421.

39 J. T. Boronski, A. E. Crumpton, L. L. Wales and S. Aldridge, Diberyllocene, a Stable Compound of Be(i) with a Be-Be Bond, *Science*, 2023, **380**, 1147–1149.

40 J. L. Dutton, A Big Breakthrough for Beryllium: A Stable Organometallic Compound with a Be-Be Bond has been Synthesized, *Science*, 2023, **380**, 1106–1107.

41 F. Weinhold, Natural Bond Critical Point Analysis: Quantitative Relationships between NBO-Based and QTAIM-Based Topological Descriptors of Chemical Bonding, *J. Comput. Chem.*, 2012, **33**, 2440–2449.